Integrated Photonic Microring Resonators for FSR Dependent Microwave Bandpass Filters

Ashitosh Velamuri,* and Bijoy Krishna Das

Centre for Programmable Photonic Integrated Circuits and Systems, Department of Electrical Engineering, IIT Madras, Chennai-600036, India

**ee18d042@smail.iitm.ac.in*

Abstract: We have proposed a uniquely designed silicon photonic microring resonator for microwave bandpass filters; FSR of the microring is key to define the centre frequency. A bandwidth tunable (1.4-4.5GHz) Ku-band filter has been demonstrated experimentally.

1. Introduction

Microwave filter is an essential building block in any microwave receiver architecture to separate the unwanted interfere from the signal of interest. The programmable microwave photonic filters show promise in terms of size, weight and power (SWaP), wide-band tunability and scalability, which are very crucial in 5G/6G networks, satellite and avionic communication systems [1]. The microring resonator (MRR) is the popular integrated photonic device to realize the RF filter operation due to its low footprint, high tunability range and better bandwidth control. However, the inherent phase response of the MRR limits the microwave bandpass filter response, resulting in asymmetric out-of-band rejection [2]. Recently, two cascaded microring resonators in all-pass configuration [2,3] and the coupled resonator optical waveguide (CROW) in add-drop configuration [4] have been used to demonstrate bandpass filters with symmetric out-of-band rejection.

In this paper we report a microwave bandpass filter at a desired centre frequency with symmetric out-of-band rejection using only a single microring resonator in all-pass configuration. It has been shown that the microring resonator can be suitably programmed to tune the bandwidth of the microwave filter.

2. Working Principle

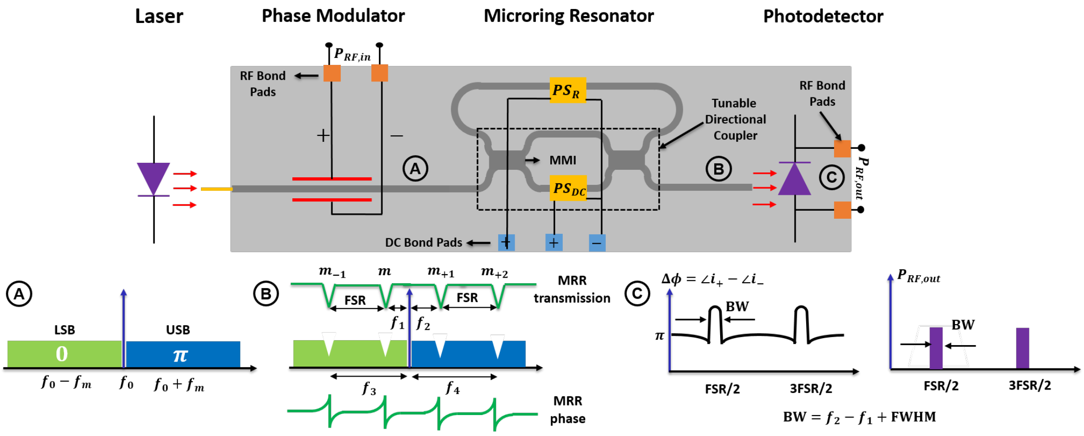

Fig. 1: Operational scheme for the proposed integrated microwave photonic bandpass filter with single microring resonator. LSB: lower sideband, USB: upper sideband, f_0, f_m are the carrier frequency and the centre of the microwave band respectively, i_+ and i_- are the photocurrents corresponding to carrier beat with the USB and carrier with the LSB respectively, $\Delta\phi$ is the phase difference between i_+ and i_-, FWHM: full-width at half maximum of the MRR.

The proposed microring resonator (MRR) design architecture and the microwave bandpass filter scheme of operation are shown in Fig. 1. The microring is designed in the all-pass configuration with a resonance tuning phase shifter PS_R and tunable coupler using a second phase shifter PS_{DC} in Mach-Zehnder interferometer (MZI) configuration. Thus, we can program the microring resonator to operate at a desired Q-value and the resonance shift with respect to the optical carrier wavelength. In this configuration, the FSR of the microring resonator is used to select the centre frequency of the microwave bandpass filter and is explained in the scheme shown in Fig. 1. The microwave bandpass filter response results from the MRR-induced phase modifications in the modulated optical spectrum at around symmetric resonance positions with respect to the optical carrier frequency ($f_1 \approx f_2$). The resonances spacing with the optical carrier (f_1, f_2) control the microwave filter's bandwidth, and the microring resonator's FSR controls the filter centre frequency $f_{c,RF}$. The resonance spacing (and the filter bandwidth) can be tuned by the integrated phase shifter PS_R. However, the tuning of the FSR is not straightforward in the conventional MRRs; therefore, the filter's central frequency remains invariant ($f_{c,RF}$ = FSR/2) in the proposed scheme. However, one can design the microwave filter for different RF frequencies by slightly altering the MRR perimeter. The required MRR perimeter to realize the microwave filter at 10 GHz (X-band), 15 GHz (Ku-band) and 26.5 GHz (K-band) are 3.5 mm, 2.3 mm and 1.4 mm, respectively. Also, the expected FSR change for the standard geometrical variation of a foundry process ($\pm$ 20 nm) is $\sim \pm$ 2 pm (250 MHz). Therefore, the proposed design tolerates fabrication imperfections, especially for high-frequency applications.

We can also note that since the MRR is designed to have low FSR and the other resonances order (m_{-1}, m_{+2}) placed at a distance f_3, f_4 (f_3+f_4 = 3FSR/2) from the optical carrier can also affect the sidebands. Therefore, the proposed scheme can be extended to realize a multi-band microwave bandpass filter at centre frequencies given by $\{(2n+1)/2\times$ FSR$\}$. The photodetector bandwidth and the waveguide dispersion limits the the number of achievable bands in the filter response. In our experiments, we have realized a single-band microwave filter due to the limitation of the detector bandwidth.

3. Experimental Results and Discussion

To realize the microwave filter with the proposed microring resonator design, a wavelength-independent tunable directional is essential to achieve the same extinction (and Q-value) for the two adjacent resonance orders . As multi-mode interferometers (MMIs) are more robust in terms of dispersion, we have chosen an MMI-based Mach-Zehnder interferometer (MZI) as the tunable coupler. For the FSR design, we have chosen the S-bend for MMI, arm length of the MZI, and waveguide bend radius in the cavity such that the perimeter of MRR is $\sim$ 2.3 mm, for which the expected FSR and the filter central frequency are $\sim$ 30 GHz and 15 GHz (Ku-band), respectively. The device was fabricated on a 220 nm silicon-on-insulator substrate at Advanced Micro Foundry (AMF) Singapore.

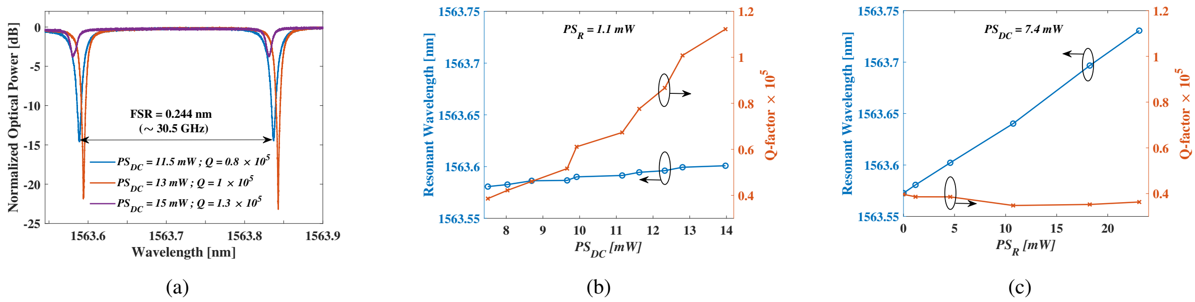

Fig. 2: (a) Thermo-optic characteristics of the fabricated MRR showing two adjacent resonance orders for different thermal power applied to PS_{DC}, (b) the change in resonant wavelength and Q-factor of the fabricated MRR with PS_{DC}, for PS_R = 1.1 mW, and (c) the change in resonant wavelength and Q-factor of the fabricated MRR with PS_R, for PS_{DC} = 7.4 mW.

Next, we have performed the thermo-optic tuning characteristics of the fabricated MRR by operating the phase shifter PS_{DC}, as shown in Fig. 2a. As expected, the change in the coupling coefficient of the MRR tunes the Q-factor and the extinction. The additional tuning of the resonant wavelength is due to adding extra phase by the heater while tuning the coupling coefficient. The free spectral range of the MRR is measured as $\sim$ 30.5 GHz (very close to the designed value of 30 GHz). After the thermo-optic measurements with one phase shifter, we have characterized the MRR with the simultaneous operation of both phase shifters. The plots of the change in resonant wavelength and the Q-factor with the simultaneous tuning of both the phase shifters are given in Fig. 2b and Fig. 2c. As expected, the Q-value (resonant wavelength) is shown to be actively tuned with PS_{DC} (PS_R), whereas it is almost constant (small increment due to tunable coupler phase) with PS_R (PS_{DC}). The measured results can be used to develop an algorithm to program the MRR characteristics (and the corresponding RF filter responses) to the desired characteristics. However, in the current experiments, we have manually tuned the coupling coefficients and the resonant wavelength for the proof-of-concept demonstration.

In the microwave filter experiments, an RF amplifier (gain = 35 dB) was used before the phase modulator to improve the link gain of the RF filter, and an erbium-doped fibre amplifier (EDFA) was used after the modulator to compensate for the fibre-to-fibre coupling loss (18 dB) of the grating coupler. A performance network analyzer (PNA) was used to sweep the RF signal from 5 GHz to 25 GHz ($P_{in,RF}$ = -30 dBm) and perform the S-parameter analysis of the microwave photonic filter. An 8-channel programmable DC power supply was used to drive the integrated phase shifters (PS_{DC} and PS_R) of the MRR. First, the MRRs coupling coefficient was tuned (PS_{DC} = 15 mW) to achieve the Q-factor of 1.3×10^5. The relative position of the resonances with the carrier was adjusted

(PS_R = 5.1 mW), such that $\Delta f = f_2 - f_1 = 765$ MHz. The corresponding measured S_{21} of the microwave photonic filter with a central frequency $f_{c,RF} \sim 15.2$ GHz is given by the dashed purple line in Fig. 3a. The 3-dB bandwidth of the filter is 1.4 GHz, and the link gain is -2.2 dB. Next, we have adjusted the thermal power to the phase shifter PS_R (5.1 - 4.1 mW) to detune the relative position of resonances with the carrier, Δf (0.76 - 1.9 GHz) and tune the 3-dB bandwidth (1.4 - 2.9 GHz) of the microwave filter, as shown in Fig. 3a. The rejection of the filter denoted as R_1 for the low-frequency range and R_2 for the high-frequency range are also marked in Fig. 3a. For the MRR Q-value of 1.3×10^5 and the filter bandwidth of 2.9 GHz, R_1 = 33.7 dB and R_2 = 29.1 dB. The contrast between the rejection values could be due to the spectral characteristics of the used experimental components (modulator, RF amplifier and/or detector) at higher frequencies. Further, we also observe that the link gain reduces for the filter responses with low bandwidth. The gain reduction is because of the perfect cancellation of the phase added by the MRR as $\Delta f \rightarrow 0$ [2].

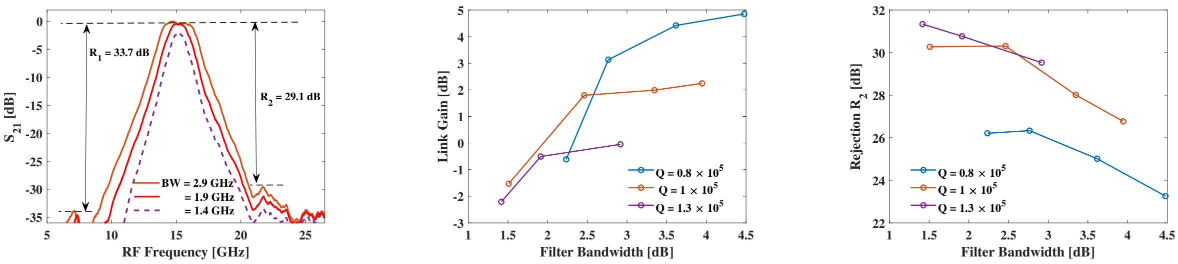

(a) (b) (c)

Fig. 3: (a) Measured RF filter response at 15.2 GHz central frequency with tunable bandwidth 1.4-2.9 GHz; (b) the link gain as a function of filter bandwidth for different Q-values of the MRR, and (c) the filter rejection as a function of filter bandwidth for different Q-values of the MRR.

To further extend the bandwidth tuning range of the RF filter, we have changed the Q-factor (coupling coefficient) of the MRR by changing the thermal power to PS_{DC}. Fig. 3b shows the link gain variation with the filter bandwidth for different Q-values of the MRR. The figure shows that the tuning range of the filter bandwidth changes with the MRR Q-factor, and the link gain shows similar behaviour (drop for narrowband filters) for all the coupling coefficients. Here, we can also note the positive values of link gain because of the pre-amplification of the RF signal before the modulator. Fig. 3c shows the filter rejection R_2 variation with the filter bandwidth, which is greater than 23 dB across the bandwidth tuning range of the filter.

4. Conclusion

We proposed a unique microring resonator design to realize the microwave filter bandpass response with symmetric out-of-band rejection. The RF filter frequency can tuned by changing by the free spectral range of the microring resonator. In this work, we have designed the free spectral range of the MRR to realize the RF filter response at $\sim$ 15 GHz (Ku-band, FSR/2). The device was fabricated at Advanced Micro Foundry (AMF), Singapore. We have performed the microwave filter experiments to validate the proposed scheme and realized the filter response around 15.2 GHz, with symmetric out-of-band rejection $\sim$ 30 dB for MRR Q = 1.3×10^5. We have adjusted the two integrated thermo-optic phase shifters to tune the Q-factor of the MRR and the resonant wavelength spacing with the optical carrier and measured the tunable filter bandwidth of 1.4 - 4.5 GHz. The out-of-band rejection is greater than 23 dB throughout the bandwidth tuning range. The proposed device can be designed for multi-band radar applications.

Acknowledgements

The authors gratefully acknowledge MeitY, Govt. of India for sponsoring NNetRA project and for the establishment of CoE-CPPICS at IIT Madras.

References

1. Liu, Y., et al. ”Integrated microwave photonic filters.” Advances in Optics and Photonics, vol. 12, no. 2, pp. 485 – 555, 2020.
2. A. Velamuri and B. K. Das, “Programmable Silicon Photonic RF Filters With Symmetric Out-of-Band Rejection,” in Journal of Lightwave Technology, doi: 10.1109/JLT.2023.3323477, 2023.
3. Cheng, Wei, et al. “Tunable bandpass microwave photonic filter with largely reconfigurable bandwidth and steep shape factor based on cascaded silicon nitride micro-ring resonators,” Optics Express, vol. 31, no. 16, pp. 25648-25661, 2023.
4. Y. Liu, Y. Yu, L. Wang, Y. Yu and X. Zhang, “Reconfigurable Microwave Photonic Bandpass Filter Based on CROW,” in Journal of Lightwave Technology, doi: 10.1109/JLT.2023.3323494, 2023.